

Federated Class-Incremental Learning with Hierarchical Generative Prototypes

Riccardo Salami^{1*}, Pietro Buzzega^{1*}, Matteo Mosconi¹, Mattia Verasani¹, Simone Calderara¹

¹ AImageLab - University of Modena and Reggio Emilia, Modena, Italy
name.surname@unimore.it

Abstract

Federated Learning (FL) aims at unburdening the training of deep models by distributing computation across multiple devices (clients) while safeguarding data privacy. On top of that, Federated Continual Learning (FCL) also accounts for data distribution evolving over time, mirroring the dynamic nature of real-world environments. While previous studies have identified Catastrophic Forgetting and Client Drift as primary causes of performance degradation in FCL, we shed light on the importance of *Incremental Bias* and *Federated Bias*, which cause models to prioritize classes that are recently introduced or locally predominant, respectively. Our proposal constrains both biases in the last layer by efficiently fine-tuning a pre-trained backbone using learnable prompts, resulting in clients that produce less biased representations and more biased classifiers. Therefore, instead of solely relying on parameter aggregation, we leverage generative prototypes to effectively balance the predictions of the global model. Our method significantly improves the current State Of The Art, providing an average increase of +7.8% in accuracy. Code to reproduce the results is provided in the suppl. material.

1 Introduction

The traditional paradigm in Deep Learning necessitates accessing large-scale datasets all at once, which hinders scalability and raises significant privacy concerns, especially when sensitive data is involved. Although distributing training across many devices could be an effective solution, there is still no effective mechanism for blending the resulting trained models into a single unified one. Federated Learning (FL) (McMahan et al. 2017) addresses this challenge through a centralized server that coordinates distributed devices, aiming to create a single unified model while minimizing communication costs.

Federated Class-Incremental Learning (FCIL) (Yoon et al. 2021; Dong et al. 2022; Zhang et al. 2023b) takes a step further and couples distributed training with Online Learning, tolerating distribution shifts in the data over time. This presents new challenges, as deep models learning online (without relying on old examples) experience severe performance degradation due to Catastrophic Forgetting (McCloskey and Cohen 1989). In FCIL, the training process unfolds in tasks, each of which shifts the data distribution by

introducing new categories. Each task is divided into communication rounds, wherein the local models train on their private data distribution. After local training, each client may transmit information to the orchestrator (server), which creates a global model and redistributes it to all clients. In the literature, some methodologies account for architectural heterogeneity (*i.e.*, heterogeneous FL (Diao, Ding, and Tarokh 2021; Kim et al. 2022b; Ilhan, Su, and Liu 2023)), while others aim to enhance the performance of local models without necessarily converging to a global one (*i.e.*, personalized FL (Collins et al. 2021; Ma et al. 2022; OH, Kim, and Yun 2022)). Instead, we follow the original FCIL setting as presented in (Dong et al. 2022), with the goal of training a single global model in a distributed way.

When incrementally learning on a sequence of tasks, the model struggles the most at differentiating classes from distinct tasks, whereas it works well at separating those within the same one. Albeit one would intuitively link such behavior to Catastrophic Forgetting, it primarily occurs because tasks are learned in isolation, and some classes are never seen simultaneously (Kim et al. 2022a). This causes a bias towards recently introduced classes (Wu et al. 2019), which we refer to as *Incremental Bias* (IB). The authors of (Luo et al. 2021) observe a similar tendency in the Federated Learning scenario: since clients train exclusively on their local datasets, they exhibit a bias towards their local label distribution. We refer to this effect as *Federated Bias* (FB).

In contrast to the well-known Client Drift (Gao et al. 2022; Karimireddy et al. 2020; Zhao et al. 2018), which causes misalignment between the clients' learned *parameters*, Federated Bias affects the clients' *responses*. Specifically, FB induces clients' outputs to diverge in different directions, mirroring the patterns of their local label distributions. Also, the strength of FB increases with growing heterogeneity, suggesting a correlation with declining performance (see Section 2). To relieve such an effect, we constrain FB to the last layer by leveraging a frozen pre-trained backbone and efficiently fine-tuning it via prompt learning (Li and Liang 2021). Ideally, prompting keeps the clients' representations close to the pre-training optimum (hence, close to each other), thus minimizing their Federated Bias. In Section 4.3, we experimentally verify that prompting leads to reduced bias in the feature space w.r.t. fine-tuning all parameters. Consequently, this confines the impact

*These authors contributed equally.
Preprint. Under review.

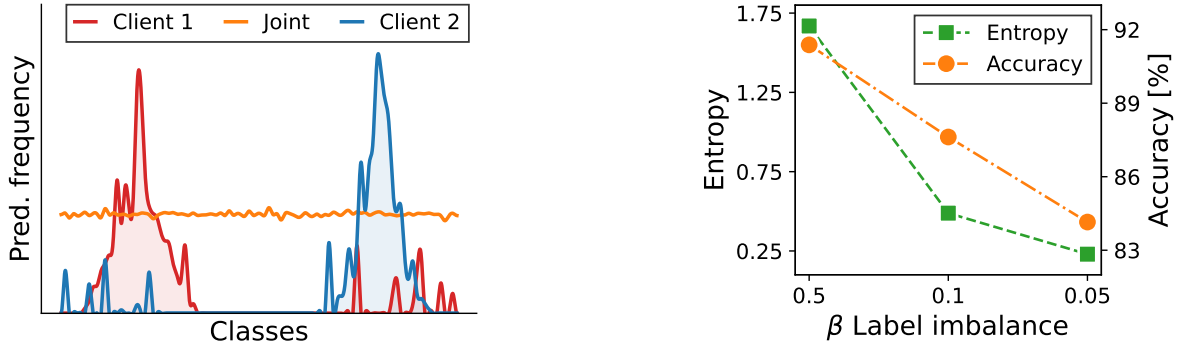


Figure 1: **Federated bias.** Histogram of the clients’ responses, computed on the global test set, for $\beta = 0.05$. Class indexes have been rearranged for improved visualization (left). The entropy of the response histograms, averaged on all clients, compared with FL performance (right).

of FB to the last layer, providing the centralized server with less biased representations. On top of that, prompt-based methodologies *i*) have demonstrated SOTA results in Class-Incremental Learning (Wang et al. 2022b,a; Smith et al. 2023) and *ii*) adapt only a small portion of the clients’ parameters, enabling unmatched communication efficiency in distributed scenarios (Zhao et al. 2023; Liu et al. 2023).

The authors of (Wu et al. 2019; Zhang et al. 2023a; Luo et al. 2021) address either IB or FB by fine-tuning the classification layer (where such biases are the most evident) on IID data samples. To meet the privacy requirements of FL, which prohibit transferring real data, we follow recent studies (Zhang et al. 2023a; Luo et al. 2021) and leverage latent generative replay. Specifically, at each communication round, we alleviate both biases – previously enforced to the last layer by the adopted prompt-based fine-tuning – by rebalancing the global classifier on a dataset of generated representations. In contrast to other approaches relying on prototypes (*i.e.*, the average feature vectors) to regularize clients’ training procedures (Tan et al. 2022; Guo et al. 2024), we propose to compute their covariance matrix and parameterize a Multivariate Gaussian distribution for each class-client combination. This forms a grid of $num_classes \times num_clients$ generative prototypes, which are sampled hierarchically (first by class, then by client) to generate new data points.

Summarizing, this work:

- sheds light on the relation between prompt learning and the aforementioned biases, identifying the latter as the primary cause of performance degradation in FCIL;
- proposes a novel methodology that confines (with prompting) and mitigates (by rebalancing) such biases in the final classification layer;
- provides a comprehensive evaluation of the proposed approach, demonstrating state-of-the-art performance on standard benchmarks while maintaining minimal communication costs.

2 On Federated Bias

This section investigates how Federated Bias in clients’ responses is associated with performance degradation in

Federated Learning. All experiments are conducted on the CIFAR-100 (Krizhevsky, Hinton et al. 2009) dataset, where the data is heterogeneously distributed across 10 clients under the commonly adopted distribution-based label imbalance setting (Li et al. 2022; Yurochkin et al. 2019).

To effectively show the presence of FB in the local models, we evaluate them at their most biased state: specifically, at the end of the local training, prior to any synchronization with the centralized server. In Figure 1 (left), we show the histogram of the responses given by two randomly selected clients, trained with $\beta = 0.05$, on the global test set. Additionally, we compare them against a model trained conventionally on the global data distribution (referred to as Joint). It can be observed that clients’ predictions are significantly skewed, mirroring their local label distribution.

To define a quantitative measure for FB, we consider the responses from all clients and compute the average entropy of the histograms of their predictions. Here, low entropy indicates a highly biased model presenting a peaked response distribution, whereas high entropy implies uniformity in the model’s responses and is linked to lower bias. The experiment is repeated for three increasingly challenging label-imbalance settings ($\beta \in \{0.5, 0.1, 0.05\}$). Figure 1 (right) shows the average entropy at the end of the local training compared to the final performance. The two curves are notably similar, suggesting a correlation between Federated Bias and performance deterioration.

3 Methodology

3.1 Problem definition

Federated Class-Incremental Learning (Zhang et al. 2023b; Guo et al. 2024) tackles a classification problem across C classes, which are introduced sequentially over T incremental tasks. For each task, the data is distributed in a non-IID manner among M clients. Let D^t be the global partition for task t , which is split among the M clients, with D_m^t being the local partition of client m at task t . The training procedure of each task is divided into communication rounds, each consisting of a certain number of epochs. At the end of the local optimization, the clients synchronize with the server by exchanging their learnable parameters. The server

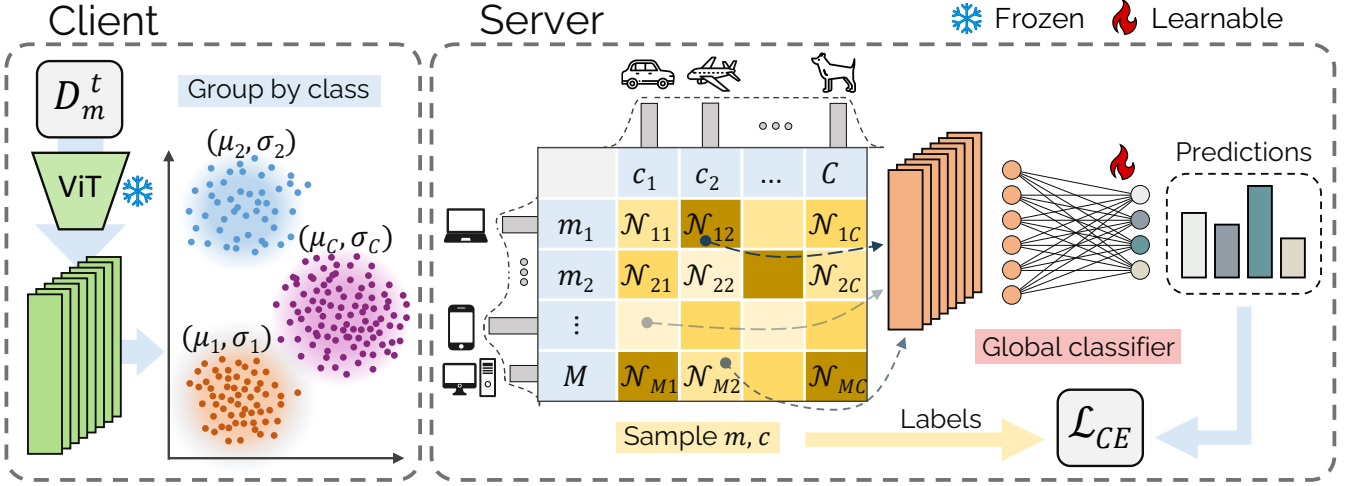


Figure 2: Classifier Rebasing procedure through hierarchical sampling.

aggregates these parameters into a global model and redistributes it to all clients, thus concluding the communication round. Since data from previous tasks is unavailable, client m can only train on its dataset D_m^t during task t . Let f_{θ_m} be the local model of client m , parameterized by θ_m . The local objective is to minimize the loss function \mathcal{L} with respect to the local dataset D_m^t , namely:

$$\underset{\theta_m}{\text{minimize}} \quad \mathbb{E}_{(x,y) \sim D_m^t} \mathcal{L}(f_{\theta_m}(x), y). \quad (1)$$

The goal of the centralized server is to find the optimal set of parameters θ that minimizes the loss function on the entire dataset, without having access to any data point:

$$\underset{\theta}{\text{minimize}} \quad \frac{1}{TM} \sum_{t=1}^T \sum_{m=1}^M \mathbb{E}_{(x,y) \sim D_m^t} \mathcal{L}(f_{\theta}(x), y). \quad (2)$$

3.2 Hierarchical Generative Prototypes

We introduce Hierarchical Generative Prototypes (HGP), which comprises two key components: i) *prompting*, reducing communication costs and constraining Federated and Incremental biases within the classifier; ii) *classifier rebalancing*, addressing these biases on the server side. We report the pseudo-code algorithm in the supplementary material.

Prompting. Differently from other prompt-based CL approaches, which rely on a *pool* of task-generic (Wang et al. 2022b) or task-specific (Smith et al. 2023; Wang et al. 2022a) prompts, we propose learning a *single* prompt shared across all tasks. This eliminates the need for prompt selection – which requires an additional forward pass – and significantly accelerates both training and inference. Specifically, we instantiate two learnable vectors, P_k and P_v , for each of the first 5 transformer blocks, obtaining the prompt $\mathcal{P} = \{P_k^j, P_v^j \mid j \in 1, \dots, 5\}$. Following prefix-tuning (Li and Liang 2021), P_k^j and P_v^j are respectively prepended to the keys and values of the j^{th} Multi-head Self Attention layer and optimized jointly to minimize the loss function.

After training on the local data distribution, each client sends its learnable parameters (consisting of prompt and classification head) to the server. Then, given $|D^t| = \sum_{m=1}^M |D_m^t|$, where $|\cdot|$ represents the cardinality of a set, the server aggregates the parameters as:

$$\theta^t = \frac{1}{|D^t|} \sum_{m=1}^M |D_m^t| \theta_m^t. \quad (3)$$

Here, $\theta_m^t = \{\mathcal{P}_m, W_m^t\}$ indicate the learnable parameters of client m during task t (comprising of prompt \mathcal{P}_m and classification head W_m^t).

Classifier Rebasing. To mitigate biases in the classification head, we employ a rebasing procedure on the server side. Specifically, we retrain the final classification layer using data entries sampled from *generative prototypes*.

The procedure starts with each client m approximating the distribution of the features h related to class c using a multivariate Gaussian $\mathcal{N}_{m,c}(\mu_{m,c}, \Sigma_{m,c})$, where $\mu_{m,c}$ is the mean and $\Sigma_{m,c}$ the covariance matrix of the feature vectors produced by its local examples belonging to class c (see Figure 2, Client). Since other studies denote $\mu_{m,c}$ as the prototype for client m and class c , we refer to $\mathcal{N}_{m,c}$ as a generative prototype, given its capability to synthesize new samples. By repeating this process across all classes and clients, we produce $M \times C$ prototypes, which need to be combined into a single generative model that best approximates the global data distribution.

For a given class c , the server receives M generative prototypes, one from each client, and seeks to identify the single distribution that best aligns with all of them. To this aim, we take the distribution that minimizes the Jensen-Shannon Divergence (JSD) (Lin 1991). Considering multiple distributions $\mathcal{Q} = \{Q_1, \dots, Q_M\}$, with importance weights $\Pi = \{\pi_1, \dots, \pi_M\}$, their JSD is defined as:

$$\text{JSD}_{\Pi}(\mathcal{Q}) = \sum_{m=1}^M \pi_m D_{\text{KL}}(Q_m || G), \quad G = \sum_{m=1}^M \pi_m Q_m, \quad (4)$$

where D_{KL} is the Kullback-Liebler divergence.

Therefore, our objective is to find a global distribution \tilde{Q}_c for the class c that optimizes:

$$\underset{\tilde{Q}_c}{\text{minimize}} \quad \sum_{m=1}^M \pi_{m,c} D_{\text{KL}} \left(\tilde{Q}_c \parallel G \right). \quad (5)$$

Notably, the optimal solution to this problem is to set \tilde{Q}_c equal to the distribution G . Since, in our case, all distributions $\{Q_1, \dots, Q_M\}$ are Gaussians, the closest distribution G is precisely defined as a Gaussian Mixture Model (GMM). Following a common practice in Federated Learning (Tan et al. 2022; McMahan et al. 2017), we assign the importance weights $\{\pi_{1,c}, \dots, \pi_{M,c}\}$ to the generative prototypes based on the number of samples from class c observed by client m .

By solving Equation 5 for all classes, we result in C GMMs, $\{\tilde{Q}_1, \dots, \tilde{Q}_C\}$, one for each class. To obtain a single generative model, we further combine them by following a similar reasoning to the one of Equation 5. This time, we consider those C class-specific GMMs as the initial distributions in Equation 4, which leads us to define the global generative model \tilde{Q} over all classes:

$$\tilde{Q} = \sum_{c=1}^C \omega_c \tilde{Q}_c, \quad \tilde{Q}_c \triangleq \sum_{m=1}^M \pi_{m,c} \mathcal{N}_{m,c}(\mu_{m,c}, \Sigma_{m,c}), \quad (6)$$

where the class-specific weights $\{\omega_1, \dots, \omega_C\}$ are set to the normalized number of samples for each class. According to Equation 5, \tilde{Q} is the distribution that most closely aligns with all class-specific GMMs: consequently, it also provides the closest match to all the initial Gaussians across every class-client combination.

When it comes to sampling from \tilde{Q} , we recall that the standard GMM sampling process consists of two steps: first, selecting a Gaussian, and then sampling from it. Expanding on this framework, we introduce an additional step, which is used to select the class-specific GMM \tilde{Q}_c from the global distribution \tilde{Q} . Specifically, as illustrated in Figure 2 (Server), our hierarchical sampling strategy draws: *i*) the class-specific GMM index (c) from a Multinomial distribution on the class weights $\{\omega_1, \dots, \omega_C\}$; *ii*) the client-specific Gaussian index (m) from a Multinomial distribution on the class-client weights $\{\pi_{1,c}, \dots, \pi_{M,c}\}$; *iii*) the synthetic feature \hat{h} from the generative prototype $\mathcal{N}_{m,c}$.

At the conclusion of each communication round, the server *i*) generates a synthetic dataset \hat{D} by sampling from \tilde{Q} ; *ii*) aggregates the clients' learnable parameters θ_m^t according to Equation 3; *iii*) rebalances the global classifier G , parameterized by W . This latter step is achieved by minimizing the Cross-Entropy (CE) loss w.r.t. \hat{D} :

$$\underset{W}{\text{minimize}} \quad \mathbb{E}_{(\hat{h}, c) \sim \hat{D}} \mathcal{L}_{\text{CE}} \left(G_W(\hat{h}), c \right). \quad (7)$$

Finally, the server redistributes the updated classifier, alongside the aggregated prompt, back to the clients, enabling them to start the next communication round.

4 Experiments

In this section, we assess the effectiveness of the proposed method, comparing it with the current State of The Art in Federated Class-Incremental Learning.

4.1 Settings

Datasets. Following (Guo et al. 2024), we evaluated the proposed method on the CIFAR-100 (Krizhevsky, Hinton et al. 2009) and Tiny-ImageNet (Le and Yang 2015) datasets. Each one is partitioned into 10 incremental tasks, resulting in 10 and 20 classes per task respectively. We distribute the data across 10 clients, employing the widely adopted *distribution-based* (Li et al. 2022; Yurochkin et al. 2019) and *quantity-based* (Li et al. 2022; McMahan et al. 2017) label imbalance settings. The former partitions the data based on a Dirichlet distribution governed by a β parameter, while the latter ensures that each client encounters exactly α classes within each task. We assess all methods across 6 scenarios for each dataset. For quantity-based label imbalance settings, we set $\alpha \in \{2, 4, 6\}$ for CIFAR-100, and $\alpha \in \{4, 8, 12\}$ for Tiny-ImageNet. On both datasets, we conduct experiments with $\beta \in \{0.05, 0.1, 0.5\}$. For all experiments, we evaluate the centralized model using the global test set.

Implementation Details. We utilize a pre-trained ViT-B/16 as the backbone for HGP and all the compared methods. Specifically, we initialize the models with supervised pre-trained weights on ImageNet-21K (Ridnik et al. 2021) for CIFAR-100 and self-supervised pre-trained weights of DINO (Caron et al. 2021) for Tiny-ImageNet. This choice is grounded on mitigating potential data leakage when adapting the model for the latter dataset, which is a subset of ImageNet (Deng et al. 2009). For a complete overview of all the hyperparameters, refer to the supplementary material. Results are averaged across 3 runs.

4.2 Results

Metrics. We assess the performance of all methods using two widely adopted metrics in FCIL literature: Final Average Accuracy (FAA) and Average Incremental Accuracy (AIA). For the mathematical definitions of these measures, we refer the reader to the supplementary material.

Evaluated approaches. Our proposal is evaluated alongside *ten* competitors, following the methodology outlined in (Guo et al. 2024). Among these, five were originally designed for Class-Incremental Learning (CIL), one for Federated Learning (FL), and the remainder four for Federated Class-Incremental Learning (FCIL). Following common practice, we adapt CIL approaches for FCIL by aggregating local models with FedAvg (McMahan et al. 2017). Instead, the FL methodology (CCVR) is adapted for FCIL by enabling it to leverage all artifacts produced across tasks.

From CIL, we include two regularization-based techniques (EWC (Kirkpatrick et al. 2017), LwF (Li and Hoiem 2017)), one leveraging a rehearsal buffer (iCaRL (Rebuffi et al. 2017)), and two prompting-based approaches (L2P (Wang et al. 2022b), CODA-Prompt (Smith et al.

Partition	$\beta = 0.5$	$\beta = 0.1$	$\beta = 0.05$	$\alpha = 6$	$\alpha = 4$	$\alpha = 2$
Joint				92.3		
EWC _{FL}	8.7 (24.5)	4.9 (13.1)	4.0 (11.3)	5.4 (17.8)	4.7 (14.4)	1.2 (6.8)
LwF _{FL}	16.3 (35.8)	7.7 (17.8)	7.7 (14.9)	11.4 (24.6)	10.3 (19.4)	3.0 (9.3)
iCaRL _{FL}	54.8 (63.7)	48.2 (53.5)	42.9 (43.8)	42.2 (48.6)	38.5 (42.3)	26.8 (28.3)
CCVR	64.2 (79.6)	63.2 (77.7)	61.3 (76.4)	65.3 (79.1)	66.4 (78.9)	51.1 (69.7)
L2P _{FL}	77.4 (83.3)	71.3 (79.4)	69.4 (77.0)	72.8 (80.3)	70.4 (79.2)	63.4 (72.0)
CODA-P _{FL}	61.3 (71.8)	18.1 (35.4)	15.9 (34.3)	35.2 (50.0)	15.1 (34.6)	27.7 (9.5)
TARGET	13.3 (33.8)	1.2 (13.6)	4.0 (12.7)	6.4 (23.9)	5.7 (18.7)	1.6 (8.2)
GLFC	– (–)	– (–)	– (–)	50.0 (66.9)	50.5 (61.0)	4.4 (12.5)
LGA	– (–)	– (–)	– (–)	62.9 (73.5)	61.4 (67.5)	9.8 (15.1)
PLoRA	79.3 (85.9)	78.2 (84.6)	77.8 (84.5)	79.2 (85.3)	77.4 (83.7)	73.2 (81.1)
HGP (ours)	89.6 (93.1)	89.7 (93.0)	89.0 (92.5)	89.6 (93.3)	89.7 (93.1)	88.4 (92.1)
Gain	+10.3 (+7.2)	+11.5 (+8.4)	+11.2 (+8.0)	+10.4 (+8.0)	+12.3 (+9.4)	+15.2 (+11.0)

Table 1: **CIFAR-100 results.** Results in terms of FAA [\uparrow] and AIA [\uparrow]. AIA is reported between parenthesis. Best results are highlighted in bold. Gain refers to the previous SOTA approach. The subscript _{FL} indicates CL methods adapted for FCIL.

2023)). From FL and FCIL, we select a rebalancing-based approach (CCVR (Luo et al. 2021)), a Parameter-Efficient Fine-Tuning technique (PLoRA (Guo et al. 2024)), two rehearsal-based methods (GLFC (Dong et al. 2022), LGA (Dong et al. 2023)), and one utilizing generative replay (TARGET (Zhang et al. 2023b)). Results for all methods, except HGP, CODA-Prompt, and CCVR, are sourced from previous research (Guo et al. 2024). Finally, we include the upper bound, established by training the same backbone jointly on the global data distribution (*i.e.*, without applying of federated or incremental splitting), referred to as Joint.

Comparison. In Tables 1 and 2, we present the results of HGP and the other approaches in terms of FAA [\uparrow] and AIA [\uparrow] on the CIFAR-100 and Tiny-ImageNet datasets, respectively. Generally, all methods tested on Tiny-ImageNet (including Joint) exhibit lower performance compared to CIFAR-100, indicating the greater challenge posed by the former dataset. Consistent with previous findings (van de Ven, Tuytelaars, and Tolias 2022; Buzzega et al. 2020), regularization techniques for CIL (EWC, LwF) perform poorly across all imbalance levels, indicating severe forgetting issues during incremental learning. iCaRL is less effective compared to prompting techniques like L2P¹ and CODA-Prompt on more balanced datasets. However, thanks to the presence of a memory buffer of old samples, it maintains relatively consistent results as label imbalance increases. Even without a buffer, CCVR also maintains stable performance thanks to its effective rebalancing strategy, providing better results than iCaRL. While L2P generally outperforms CODA-Prompt, its performance remains lower than PEFT-based methods designed specifically for FCIL.

Among FCIL methods, TARGET exhibits the lowest performance. Notably, it exhibits significantly higher AIA compared to FAA, suggesting ineffective mitigation of forgetting

through its generative replay. GLFC and LGA² perform better than iCaRL but worse than prompting techniques, indicating the improved effectiveness of their class-aware gradient compensation compared to relying solely on a memory buffer. However, both methods struggle with highly imbalanced label distributions.

PEFT-based methods specifically designed for FCIL (PLoRA, HGP) outperform other methodologies across all settings. The use of prototypes enables them to handle increasing label imbalance more effectively, resulting in the most stable performance among variations in α and β in both datasets. HGP significantly outperforms PLoRA in all scenarios by leveraging generative prototypes on the centralized server, demonstrating superior robustness to both incremental and federated biases.

4.3 Ablation study

Prompting vs. fine-tuning. In this section, we explore the impact of prompting on Federated Bias, emphasizing the contrast with the traditional approach of fine-tuning the whole network. All experiments are performed on the CIFAR-100 dataset, distributed across 10 clients under different distribution-based label imbalance settings.

We argue that prompting is a more advantageous approach for adapting pre-trained models in Federated Learning, as it constrains the bias to the last layer instead of distributing it across the whole network. To experimentally prove this claim, we position ourselves at the end of the local training prior to the first synchronization with the server: namely, when each client is trained exclusively on its local distribution. In this scenario, we assess the Federated Bias within the feature space – which we refer to as *feature bias* for short – by computing the local prototypes for the 10 clients and measuring their average pairwise Euclidean dis-

¹For further insights on L2P results, we refer the reader to the supplementary material.

²Due to computing constraints, we omit the performance of GLFC and LGA on distribution-based label imbalance settings.

Partition	$\beta = 0.5$	$\beta = 0.1$	$\beta = 0.05$	$\alpha = 12$	$\alpha = 8$	$\alpha = 4$
Joint	84.3					
CCVR	56.4 (71.7)	58.6 (72.2)	56.3 (69.8)	55.4 (71.6)	55.6 (71.7)	57.2 (70.4)
L2P _{FL}	64.2 (66.9)	56.3 (52.5)	51.9 (43.2)	61.6 (58.0)	49.4 (39.3)	8.2 (10.2)
CODA-P _{FL}	72.2 (81.1)	54.4 (64.2)	45.6 (57.9)	64.3 (75.1)	49.9 (62.2)	27.1 (42.8)
TARGET	7.7 (20.5)	0.5 (8.7)	0.9 (5.3)	3.5 (17.6)	4.1 (16.4)	0.5 (4.8)
GLFC	– (–)	– (–)	– (–)	35.0 (47.9)	20.2 (37.5)	5.1 (8.7)
LGA	– (–)	– (–)	– (–)	37.3 (53.2)	61.4 (67.5)	6.5 (9.8)
PLoRA	75.5 (81.8)	74.3 (81.0)	74.1 (80.7)	75.3 (81.7)	75.2 (81.6)	73.6 (80.1)
HGP (ours)	78.6 (84.9)	78.6 (84.8)	78.1 (84.8)	78.4 (84.8)	78.4 (84.8)	78.2 (84.4)
Gain	+3.1 (+3.1)	+4.3 (+3.8)	+4.0 (+4.1)	+3.1 (+3.1)	+3.2 (+3.2)	+4.6 (+4.3)

Table 2: **Tiny-ImageNet results.** Results in terms of FAA [\uparrow] and AIA [\uparrow]. AIA is reported between parenthesis. Best results are highlighted in bold. Gain refers to the previous SOTA approach. The subscript _{FL} indicates CL methods adapted for FCIL.

Prompting	CR _{old}	CR _{cur}	CIFAR-100	Tiny-ImageNet
✗	✗	✗	44.8	38.7
✓	✗	✗	51.8	43.5
✓	✓	✗	81.7	70.7
✓	✗	✓	77.8	69.8
✓	✓	✓	88.9	78.7

Table 3: **HGP components.** Evaluation of the singular components of HGP in terms of FAA [\uparrow].

tance. Figure 3 (left) shows that prompting results in smaller feature bias compared to traditional fine-tuning, suggesting that the obtained features are less biased towards the local distributions. To validate this assertion, we also compute the same metric on the pre-trained model (ViT-B-16 on ImageNet-21k), which yields the smallest bias by design. This further supports our reasoning, as this last network experiences no fine-tuning whatsoever.

On the right-hand side of Figure 3, we show the performance of prompting *vs.* traditional fine-tuning. In line with recent works (Zhang et al. 2023a; Panos et al. 2023; McDonnell et al. 2024), prompting (Prompt) shows inferior performance compared to fine-tuning, due to its limited plasticity. However, when leveraging Classifier Rebalancing (CR) on both approaches, we observe a reversal in this trend. Notably, simply addressing Federated Bias in the last layer is sufficient for prompting to outperform classical fine-tuning: this suggests that prompting techniques train more biased classifiers while producing less biased features, effectively restricting FB to the final layer.

Impact of Different Components. We assess the specific contributions of various components of HGP in terms of FAA for both benchmarks under one distribution-based label imbalance setting with $\beta = 0.05$. Results of these ablative experiments are summarized in Table 3.

Starting with the full fine-tuning of ViT-B/16 serves as a lower bound. Incorporating our prompting technique yields a notable improvement. It is worth noting that the primary advantage of prompting lies not only in enhancing accuracy

but also in confining bias to the final classification layer, thereby facilitating Classifier Rebalancing.

We denote CR_{cur} and CR_{old} as the classifier rebalancing procedure applied to the current task classes and the old tasks classes, respectively. Specifically, CR_{cur} rebalances the classifier with features generated from prototypes belonging to the set of classes of the current task, while CR_{old} employs sampling on the set of classes of the old tasks. The latter performs better than the former, indicating the greater importance of addressing Incremental Bias.

By integrating all components, HGP achieves state-of-the-art performance as reported in Tables 1 and 2.

5 Relation with prior works

Federated Learning. In its most naive form, Federated Learning suggests combining local models at the conclusion of each round through parameters averaging (McMahan et al. 2017). Other approaches introduce regularization techniques during local models’ training to prevent them from drifting too far from the server’s parameter space. For instance, FedProx (Li et al. 2020) and SCAFFOLD (Karimireddy et al. 2020) enforce such regularization. FedDC (Gao et al. 2022) estimates the local parameter shift and employs it as a correction term before aggregating parameters. GradMA (Luo et al. 2023) addresses optimization challenges (*i.e.*, quadratic programming) by rerouting each client update towards optimizing the local problem while maintaining proximity to the server. On a different trajectory, FedProto (Tan et al. 2022) computes prototypes for each class observed by each client, which are then aggregated by the server into global prototypes, serving as target representations for subsequent rounds. Similarly, in (Luo et al. 2021), the authors fit Gaussian distributions for each class and use them to generate an IID dataset of features, subsequently calibrating the server’s classification head with these features. In our work, we leverage hierarchical Gaussian Mixture Models (GMMs) of prototypes and sample from them to rebalance the global classifier.

Class-Incremental Learning. Class-Incremental Learning (CIL) stands out as one of the most challenging set-

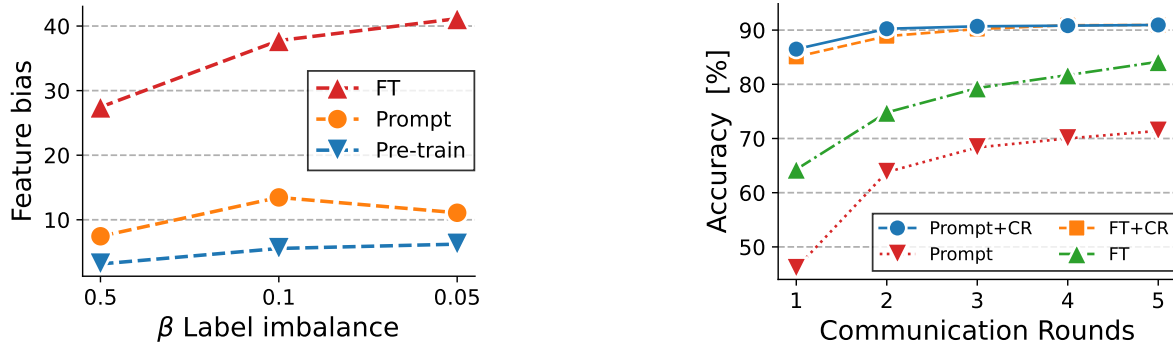


Figure 3: **Prompting vs. fine-tuning.** Average pairwise distance of the local prototypes on all clients (left). FL performance before and after Classifier Rebalancing (CR), for $\beta = 0.05$ (right).

tings within the Continual Learning domain (van de Ven, Tuytelaars, and Tolias 2022). In this scenario, the training process is divided into distinct tasks, each introducing new classes as the training progresses. To address this setting, early methods rely on regularization techniques, establishing checkpoints for previous tasks and aiming to maintain proximity w.r.t. their parameters (Zenke, Poole, and Ganguli 2017; Kirkpatrick et al. 2017) or predictions (Li and Hoiem 2017). Alternatively, rehearsal-based approaches involve storing samples in a limited memory buffer and subsequently replaying them to optimize either the original objective (Robins 1995; Chaudhry et al. 2018) or a different one based on knowledge distillation (Rebuffi et al. 2017; Buzzega et al. 2020). The emergence of pre-trained self-attentive architectures (Dosovitskiy et al. 2020) in the Computer Vision domain has paved the way for significant advancements, particularly with the advent of Parameter-Efficient Fine-Tuning (PEFT) techniques. Notably, recent approaches (Wang et al. 2022b,a; Smith et al. 2023) have harnessed prompting to achieve state-of-the-art performance in CIL, eliminating the need for a buffer to replay old samples. Instead, they employ a prompt pool comprising incrementally learned prompts, utilized to condition the network during the forward pass. In our method, we embrace the prompting paradigm, which not only delivers robust performance but also facilitates efficient communication rounds in terms of exchanged parameters.

Federated Class-Incremental Learning. The concept of Federated Class-Incremental Learning (FCIL) was initially introduced in (Yoon et al. 2021). In their work, the authors propose FedWeIT, which partitions client-side parameters into task-generic and task-specific components. To mitigate interference between clients, they implement sparse learnable masks to selectively extract relevant knowledge for each client. GLFC (Dong et al. 2022) takes a different approach by combining local buffers with class-aware gradient compensation loss. This strategy helps counteract catastrophic forgetting through rehearsal, while also adjusting the magnitude of gradient updates based on whether input samples belong to new or old classes. Building upon this framework, an enhanced version is introduced by the same authors in the LGA paper (Dong et al. 2023). TARGET (Zhang et al.

2023b) tackles forgetting by training a centralized generator network to produce synthetic data, maintaining a similar behavior to the generator used in previous tasks. The generative network populates a buffer after each task, allowing clients to utilize it for rehearsal. Recent advancements in FCIL involve fine-tuning pre-trained models using PEFT techniques. Fed-CPrompt (Bagwe et al. 2023) introduces a regularization term that encourages local prompts to diverge from global ones, enabling them to learn task-specific features. Meanwhile, PLoRA (Guo et al. 2024) integrates LoRA (Hu et al. 2021) with prototypes, which are aggregated via a re-weighting mechanism on the server side during each communication round. As a result, clients leverage these aggregated prototypes as target representations to govern local training.

6 Conclusions

In this work, we propose Hierarchical Generative Prototypes (HGP), an approach aimed at mitigating Incremental and Federated Biases within Federated Class-Incremental Learning. HGP utilizes pre-trained architectures conditioned by prompting to achieve communication efficiency. We examine the bias implications of fine-tuning the entire model compared to using prompting techniques, demonstrating that prompting confines the bias primarily to the classification layer. Building on these insights, we propose Classifier Rebalancing as a solution. This method involves sampling features from a hierarchical Gaussian Mixture Model to train the classifier across all observed classes, effectively reducing bias in the classification layer. Through the integration of prompt learning and Classifier Rebalancing, we achieve superior performance compared to the State of The Art while transmitting only a minimal number of parameters.

Limitations and Future Works. This work builds upon Prompt Learning, which effectively manages communication costs and Federated Bias while preserving adaptability. However, although leveraging a pre-trained model is a common strategy in Federated Learning literature (Guo et al. 2024; Liu et al. 2023; Bagwe et al. 2023), our findings may not extend to scenarios where models are trained from scratch. We leave the exploration of how other PEFT techniques impact federated bias to future research.

References

Bagwe, G.; Yuan, X.; Pan, M.; and Zhang, L. 2023. FedCPrompt: Contrastive Prompt for Rehearsal-Free Federated Continual Learning. In *Federated Learning and Analytics in Practice: Algorithms, Systems, Applications, and Opportunities*.

Buzzega, P.; Boschini, M.; Porrello, A.; Abati, D.; and Calderara, S. 2020. Dark experience for general continual learning: a strong, simple baseline. *Advances in Neural Information Processing Systems*.

Caron, M.; Touvron, H.; Misra, I.; Jégou, H.; Mairal, J.; Bojanowski, P.; and Joulin, A. 2021. Emerging properties in self-supervised vision transformers. In *IEEE International Conference on Computer Vision*.

Chaudhry, A.; Ranzato, M.; Rohrbach, M.; and Elhoseiny, M. 2018. Efficient Lifelong Learning with A-GEM. In *International Conference on Learning Representations*.

Collins, L.; Hassani, H.; Mokhtari, A.; and Shakkottai, S. 2021. Exploiting shared representations for personalized federated learning. In *International Conference on Machine Learning*.

Deng, J.; Dong, W.; Socher, R.; Li, L.-J.; Li, K.; and Fei-Fei, L. 2009. Imagenet: A large-scale hierarchical image database. In *Proceedings of the IEEE Conference on Computer Vision and Pattern Recognition*.

Diao, E.; Ding, J.; and Tarokh, V. 2021. HeteroFL: Computation and Communication Efficient Federated Learning for Heterogeneous Clients. In *International Conference on Learning Representations*.

Dong, J.; Li, H.; Cong, Y.; Sun, G.; Zhang, Y.; and Van Gool, L. 2023. No one left behind: Real-world federated class-incremental learning. *IEEE Transactions on Pattern Analysis and Machine Intelligence*.

Dong, J.; Wang, L.; Fang, Z.; Sun, G.; Xu, S.; Wang, X.; and Zhu, Q. 2022. Federated class-incremental learning. In *Proceedings of the IEEE Conference on Computer Vision and Pattern Recognition*.

Dosovitskiy, A.; Beyer, L.; Kolesnikov, A.; Weissenborn, D.; Zhai, X.; Unterthiner, T.; Dehghani, M.; Minderer, M.; Heigold, G.; Gelly, S.; et al. 2020. An Image is Worth 16x16 Words: Transformers for Image Recognition at Scale. In *International Conference on Learning Representations*.

Gao, L.; Fu, H.; Li, L.; Chen, Y.; Xu, M.; and Xu, C.-Z. 2022. Feddc: Federated learning with non-iid data via local drift decoupling and correction. In *Proceedings of the IEEE Conference on Computer Vision and Pattern Recognition*.

Guo, H.; Zhu, F.; Liu, W.; Zhang, X.-Y.; and Liu, C.-L. 2024. Federated Class-Incremental Learning with Prototype Guided Transformer. *arXiv preprint arXiv:2401.02094*.

Hu, E. J.; Wallis, P.; Allen-Zhu, Z.; Li, Y.; Wang, S.; Wang, L.; Chen, W.; et al. 2021. LoRA: Low-Rank Adaptation of Large Language Models. In *International Conference on Learning Representations*.

Ilhan, F.; Su, G.; and Liu, L. 2023. Scalefl: Resource-adaptive federated learning with heterogeneous clients. In *Proceedings of the IEEE Conference on Computer Vision and Pattern Recognition*.

Jung, D.; Han, D.; Bang, J.; and Song, H. 2023. Generating instance-level prompts for rehearsal-free continual learning. In *IEEE International Conference on Computer Vision*.

Karimireddy, S. P.; Kale, S.; Mohri, M.; Reddi, S.; Stich, S.; and Suresh, A. T. 2020. Scaffold: Stochastic controlled averaging for federated learning. In *International Conference on Machine Learning*.

Kim, G.; Xiao, C.; Konishi, T.; Ke, Z.; and Liu, B. 2022a. A theoretical study on solving continual learning. *Advances in Neural Information Processing Systems*.

Kim, M.; Yu, S.; Kim, S.; and Moon, S.-M. 2022b. DepthFL: Depthwise federated learning for heterogeneous clients. In *International Conference on Learning Representations*.

Kingma, D.; and Ba, J. 2015. Adam: A Method for Stochastic Optimization. In *International Conference on Learning Representations*.

Kirkpatrick, J.; Pascanu, R.; Rabinowitz, N.; Veness, J.; Desjardins, G.; Rusu, A. A.; Milan, K.; Quan, J.; Ramalho, T.; Grabska-Barwinska, A.; et al. 2017. Overcoming catastrophic forgetting in neural networks. *Proceedings of the National Academy of Sciences*.

Krizhevsky, A.; Hinton, G.; et al. 2009. Learning multiple layers of features from tiny images. *Master's thesis, Department of Computer Science, University of Toronto*.

Le, Y.; and Yang, X. 2015. Tiny imagenet visual recognition challenge. *CS 231N*.

Li, Q.; Diao, Y.; Chen, Q.; and He, B. 2022. Federated learning on non-iid data silos: An experimental study. In *IEEE International Conference on Data Engineering*.

Li, T.; Sahu, A. K.; Zaheer, M.; Sanjabi, M.; Talwalkar, A.; and Smith, V. 2020. Federated optimization in heterogeneous networks. *Proceedings of Machine Learning and Systems*.

Li, X. L.; and Liang, P. 2021. Prefix-Tuning: Optimizing Continuous Prompts for Generation. In *Proceedings of the International Joint Conference on Natural Language Processing*.

Li, Z.; and Hoiem, D. 2017. Learning without forgetting. *IEEE Transactions on Pattern Analysis and Machine Intelligence*.

Lin, J. 1991. Divergence measures based on the Shannon entropy. *IEEE Transactions on information theory*.

Liu, C.; Qu, X.; Wang, J.; and Xiao, J. 2023. FedET: a communication-efficient federated class-incremental learning framework based on enhanced transformer. In *International Joint Conference on Artificial Intelligence*.

Luo, K.; Li, X.; Lan, Y.; and Gao, M. 2023. GradMA: A Gradient-Memory-based Accelerated Federated Learning with Alleviated Catastrophic Forgetting. In *Proceedings of the IEEE Conference on Computer Vision and Pattern Recognition*.

Luo, M.; Chen, F.; Hu, D.; Zhang, Y.; Liang, J.; and Feng, J. 2021. No fear of heterogeneity: Classifier calibration for federated learning with non-iid data. *Advances in Neural Information Processing Systems*.

Ma, X.; Zhang, J.; Guo, S.; and Xu, W. 2022. Layer-wised model aggregation for personalized federated learning. In *Proceedings of the IEEE Conference on Computer Vision and Pattern Recognition*.

McCloskey, M.; and Cohen, N. J. 1989. Catastrophic interference in connectionist networks: The sequential learning problem. In *Psychology of learning and motivation*.

McDonnell, M. D.; Gong, D.; Parvaneh, A.; Abbasnejad, E.; and van den Hengel, A. 2024. Ranpac: Random projections and pre-trained models for continual learning. *Advances in Neural Information Processing Systems*.

McMahan, B.; Moore, E.; Ramage, D.; Hampson, S.; and y Arcas, B. A. 2017. Communication-efficient learning of deep networks from decentralized data. In *International Conference on Artificial Intelligence and Statistics*.

OH, J. H.; Kim, S.; and Yun, S. 2022. FedBABU: Toward Enhanced Representation for Federated Image Classification. In *International Conference on Learning Representations*.

Panos, A.; Kobe, Y.; Reino, D. O.; Aljundi, R.; and Turner, R. E. 2023. First Session Adaptation: A Strong Replay-Free Baseline for Class-Incremental Learning. In *IEEE International Conference on Computer Vision*.

Rebuffi, S.-A.; Kolesnikov, A.; Sperl, G.; and Lampert, C. H. 2017. icarl: Incremental classifier and representation learning. In *Proceedings of the IEEE Conference on Computer Vision and Pattern Recognition*.

Ridnik, T.; Ben-Baruch, E.; Noy, A.; and Zelnik-Manor, L. 2021. ImageNet-21K Pretraining for the Masses. In *Conference on Neural Information Processing Systems Datasets and Benchmarks Track (Round 1)*.

Robins, A. 1995. Catastrophic forgetting, rehearsal and pseudorehearsal. *Connection Science*.

Smith, J. S.; Karlinsky, L.; Gutta, V.; Cascante-Bonilla, P.; Kim, D.; Arbelle, A.; Panda, R.; Feris, R.; and Kira, Z. 2023. CODA-Prompt: COntinual Decomposed Attention-based Prompting for Rehearsal-Free Continual Learning. In *Proceedings of the IEEE Conference on Computer Vision and Pattern Recognition*.

Tan, Y.; Long, G.; Liu, L.; Zhou, T.; Lu, Q.; Jiang, J.; and Zhang, C. 2022. Fedproto: Federated prototype learning across heterogeneous clients. In *Proceedings of the AAAI Conference on Artificial Intelligence*.

van de Ven, G. M.; Tuytelaars, T.; and Tolias, A. S. 2022. Three types of incremental learning. *Nature Machine Intelligence*.

Wang, Z.; Zhang, Z.; Ebrahimi, S.; Sun, R.; Zhang, H.; Lee, C.-Y.; Ren, X.; Su, G.; Perot, V.; Dy, J.; et al. 2022a. Dual-prompt: Complementary prompting for rehearsal-free continual learning. In *Proceedings of the European Conference on Computer Vision*.

Wang, Z.; Zhang, Z.; Lee, C.-Y.; Zhang, H.; Sun, R.; Ren, X.; Su, G.; Perot, V.; Dy, J.; and Pfister, T. 2022b. Learning to prompt for continual learning. In *Proceedings of the IEEE Conference on Computer Vision and Pattern Recognition*.

Wu, Y.; Chen, Y.; Wang, L.; Ye, Y.; Liu, Z.; Guo, Y.; and Fu, Y. 2019. Large scale incremental learning. In *Proceedings of the IEEE Conference on Computer Vision and Pattern Recognition*.

Yoon, J.; Jeong, W.; Lee, G.; Yang, E.; and Hwang, S. J. 2021. Federated continual learning with weighted inter-client transfer. In *International Conference on Machine Learning*.

Yurochkin, M.; Agarwal, M.; Ghosh, S.; Greenewald, K.; Hoang, N.; and Khazaeni, Y. 2019. Bayesian nonparametric federated learning of neural networks. In *International Conference on Machine Learning*.

Zenke, F.; Poole, B.; and Ganguli, S. 2017. Continual learning through synaptic intelligence. In *International Conference on Machine Learning*.

Zhang, G.; Wang, L.; Kang, G.; Chen, L.; and Wei, Y. 2023a. Slca: Slow learner with classifier alignment for continual learning on a pre-trained model. In *IEEE International Conference on Computer Vision*.

Zhang, J.; Chen, C.; Zhuang, W.; and Lyu, L. 2023b. Target: Federated class-continual learning via exemplar-free distillation. In *IEEE International Conference on Computer Vision*.

Zhao, H.; Du, W.; Li, F.; Li, P.; and Liu, G. 2023. Fed-prompt: Communication-efficient and privacy-preserving prompt tuning in federated learning. In *IEEE International Conference on Acoustics, Speech and Signal Processing*.

Zhao, N.; Wu, Z.; Lau, R. W.; and Lin, S. 2020. What Makes Instance Discrimination Good for Transfer Learning? In *International Conference on Learning Representations*.

Zhao, Y.; Li, M.; Lai, L.; Suda, N.; Civin, D.; and Chandra, V. 2018. Federated learning with non-iid data. *arXiv preprint arXiv:1806.00582*.

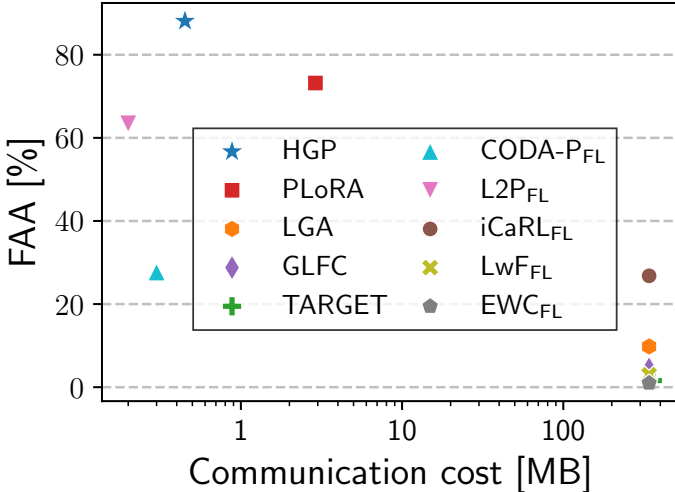


Figure A: FAA [%] in relation with the communication cost [MB] for all the tested approaches (left). Communication costs for client-server ($C \rightarrow S$) and server-client communications ($S \rightarrow C$), for each communication round (right).

A Communication cost

Efficient communication is paramount in Federated Learning because of the extensive coordination required between server and clients. In this section, we analyze the communication cost for each tested method. Figure A (left) illustrates the relationship between Final Average Accuracy (FAA) and communication cost for each method. The FAA results are derived from a quantity-based scenario with $\alpha = 2$ on Tiny-ImageNet. The communication cost (reported in Figure A, right) is measured in Megabytes (MB) per communication round and represents the average data exchanged between a single client and the server ($C \rightarrow S$) and from the server to a single client ($S \rightarrow C$).

Notably, methods that do not utilize PEFT techniques incur significantly higher communication costs, as they optimize all parameters. Consequently, with larger models, communication costs escalate proportionally without corresponding performance gains. TARGET is the most expensive method overall because the server sends the entire model and the generated dataset to clients once per task. In contrast, the adoption of PEFT techniques enhances both efficiency and performance. L2P emerges as the most efficient method, using fewer prompts than its competitors. While CODA-P transmits slightly more parameters than L2P, it keeps communication costs comparable by only transmitting prompts for the current task and freezing the rest.

PLoRA is less efficient than prompt-based methods due to the larger size of LoRA modules. However, it still achieves costs that are two orders of magnitude lower than fine-tuning approaches while delivering superior performance. HGP demonstrates efficiency on par with the other prompt-based techniques, with slightly higher server-client communication cost. This is attributed to the Classifier Rebalancing process, which also changes the classification heads related to the previous tasks, thus necessitating to communicate the whole updated classifier back to the clients.

Overall, the efficiency gains and substantial performance

Methods	$C \rightarrow S$	$S \rightarrow C$
EWC _{FL}	340.7	340.7
LwF _{FL}	340.7	340.7
iCaRL _{FL}	340.7	340.7
L2P _{FL}	0.2	0.2
CODA-P _{FL}	1.5	1.5
CCVR	340.8	340.7
TARGET	340.7	377.5
GLFC	340.7	340.7
LGA	340.7	340.7
PLoRA	2.9	2.9
HGP (ours)	1.5	1.8

improvements offered by PEFT techniques highlight their advantage in Federated Learning scenarios.

B Implementation details

B.1 Hyperparameters

We utilize a pre-trained ViT-B/16 as the backbone for HGP and all the compared methods. Specifically, we initialize the models with supervised pre-trained weights on ImageNet-21K (Ridnik et al. 2021) for CIFAR-100 and self-supervised pre-trained weights from DINO (Caron et al. 2021) for Tiny-ImageNet. This selection is made to mitigate potential data leakage when adapting the model to the latter dataset, which is a subset of ImageNet (Deng et al. 2009).

In our method, we adopt a prompt pool composed of 10 prompts for each task. Across all experiments, prompt components have a shape of $(8, d)$, where $d = 768$ represents the embedding dimension for the chosen architecture. We apply these prompts using prefix tuning, conditioning the first 5 layers of the backbone. For each task, we perform five communication rounds, during which clients observe their local datasets for five epochs with a batch size of 64. Training is conducted using the Adam optimizer (Kingma and Ba 2015) with a learning rate of 0.001; β_1 and β_2 are set to 0.9 and 0.999, respectively. A cosine annealing scheduler is employed to decay the learning rate during local training.

The centralized server rebalances the global classifier for five epochs. We use the SGD optimizer with a learning rate of 0.01 and a momentum of 0.9, with a batch size of 256, and also apply a cosine annealing learning rate scheduler. We generate an average of 256 feature vectors for each class encountered up to this point, multiplying the covariance associated with each prototype by 3 to enhance dataset diversity. All images are resized to 224×224 using bicubic interpolation and scaled to ensure their values fall within the range $[0, 1]$. Additionally, we employ random cropping and horizontal flipping as data augmentation techniques. All ex-

Partition	$\beta = 0.5$	$\beta = 0.1$	$\beta = 0.05$	$\alpha = 6$	$\alpha = 4$	$\alpha = 2$
Dataset						
L2P _{FL} (BP)	77.4 (83.3)	71.3 (79.4)	69.4 (77.0)	72.8 (80.3)	70.4 (79.2)	63.4 (72.0)
L2P _{FL}	80.0 (83.7)	47.9 (57.7)	43.2 (52.1)	49.8 (60.1)	25.2 (41.9)	10.0 (24.3)
Dataset						
Tiny-ImageNet						
L2P _{FL} (BP)	64.2 (66.9)	56.3 (52.5)	51.9 (43.2)	61.6 (58.0)	49.4 (39.3)	8.2 (10.2)
L2P _{FL}	60.3 (70.8)	42.2 (50.6)	36.5 (45.4)	51.4 (61.5)	26.8 (43.0)	7.5 (13.1)

Table A: **Batch-wise prompting.** FAA [\uparrow] and AIA [\uparrow] for L2P, with and without batch-wise prompting at test time on all settings. AIA is reported between parenthesis.

periments are conducted on a single Nvidia RTX5000 GPU.

B.2 Metrics

We assess the performance of all methods using two widely adopted metrics in FCIL literature: Final Average Accuracy (FAA) and Average Incremental Accuracy (AIA).

FAA represents the mean accuracy on all observed tasks at the conclusion of the incremental training process. Mathematically, if A_i^j denotes the accuracy on the i^{th} task at the j^{th} incremental step, where $i \leq j$, FAA can be expressed as:

$$\text{FAA} = \frac{1}{T} \sum_{i=1}^T A_i^T.$$

On the other hand, AIA provides insight into the performance progression throughout the training process. It calculates the average accuracy after each task, considering all data encountered up to that point. After completion of the entire training procedure, the mean of all measurements is computed as follows:

$$\text{AIA} = \frac{1}{T} \sum_{j=1}^T \left[\frac{1}{j} \sum_{i=1}^j A_i^j \right].$$

C Batch-wise prompting

To maintain consistency with other studies, in the main paper we report L2P performance using Batch-wise Prompting (BP) at test time (Jung et al. 2023; Smith et al. 2023). Such a procedure involves selecting the same set of prompts for all samples within a single batch during testing, thus violating the test assumption of processing each sample independently. This gives L2P an unfair advantage compared to other methods when the test dataset is not shuffled: *i.e.*, when the ground-truth labels of the examples within a single batch are typically the same.

In this respect, Table A presents L2P’s performance with and without batch-wise prompting. Without BP, the set of prompts is selected individually for each sample, ensuring independent predictions. L2P achieves similar results with and without batch-wise prompting when $\beta = 0.5$. However, in all the other settings, batch-wise prompting appears to increment L2P’s performance considerably, especially on CIFAR-100.

D Prototypes of features are privacy-preserving

In Federated Learning, maintaining the privacy of local data distributions is of utmost importance. It is crucial that no private samples are directly transmitted from the client to the server. In the HGP framework, each client provide the server with a generative prototype for each observed class.

To verify the safety of generative prototypes, we firstly examine a hypothetical scenario where an attacker gains access to the trained model along with a real image utilized during training. In such a case, the attacker could potentially employ the feature inversion technique outlined in (Zhao et al. 2020). This methodology provides for training a autoencoder to precisely match the input image. Specifically, the autoencoder takes fixed noise as input and reconstructs the image. Then, both the real and reconstructed image are passed through the frozen backbone. The objective is to minimize the mean squared error (MSE) loss between their respective features. Figure B (left) shows the real training image from the Tiny-ImageNet dataset, while Figure B (center) displays the reconstruction obtained by the trained autoencoder. Through this process, no significant semantics can be recovered. At most, the class might be guessed, but the image does not provide any detail of the original sample.

In another setting, we suppose that the attacker gains access to the centralized server, which has visibility into clients’ generative prototypes. To recover an input image, initial random noise in the input space is optimized by minimizing MSE between its features and those of a fixed sample from the generative prototype. Figure B (right) shows that this results in a shapeless, noisy reconstruction, making it impracticable for an attacker to recreate real images from these feature distributions.

E Algorithm

Algorithm 1 provides the pseudo-code for a generic task t in the HGP framework.

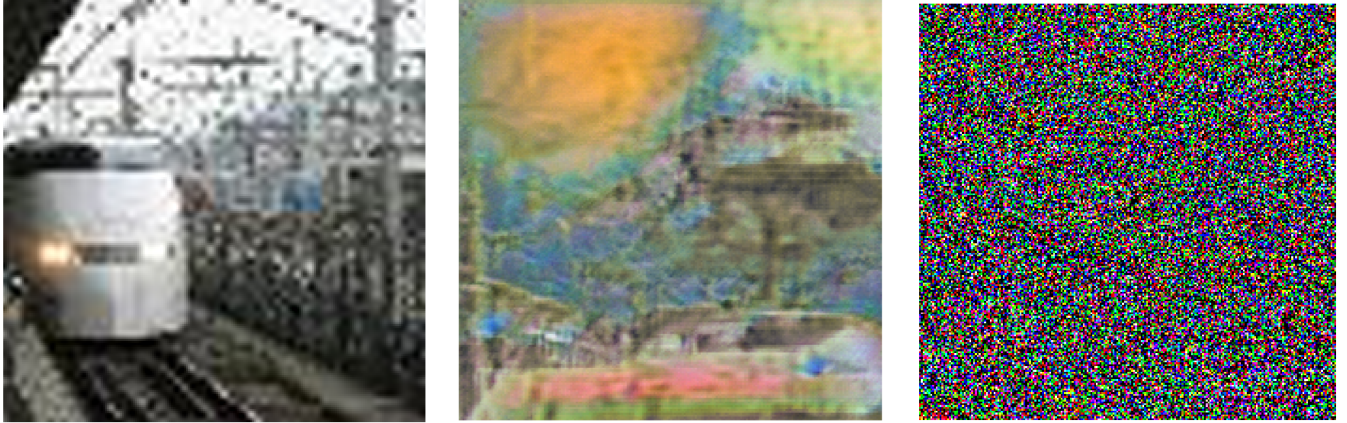


Figure B: Real training image (left) and its reconstructions leveraging either the input image (center) or the generative prototype of the related class (right).

Algorithm 1: Hierarchical Generative Prototypes **HGP**

```

1: Input: generic task  $t$ ;  $M$  clients; local model  $f_{\theta_m^t}(\cdot)$  parameterized by  $\theta_m^t = \{\mathcal{P}_m, W_m^t\}$ ;  $N$  prompts;  $C$  classes;  $E$  local
   epochs;  $E_r$  rebalancing epochs; local learning rate  $\eta$ ; rebalancing learning rate  $\eta_r$ .
2: for each communication round do
3:   Server side:
4:     Server distributes  $\theta^t$ 
5:   Client side:
6:     for each client  $m \in \{1, \dots, M\}$  in parallel do
7:        $\theta_m^t = \theta^t$ 
8:       for each local epoch  $e \in \{1, \dots, E\}$  do
9:         for each batch  $(x, y) \sim D_m^t$  do
10:           $\theta_m^t \leftarrow \theta_m^t - \eta \nabla \mathcal{L}_{\text{CE}}(f_{\theta_m^t}(x), y)$ 
11:        end for
12:      end for
13:      Compute feature vectors  $h$  on  $D_m^t$ 
14:      for each class  $c \in C^t$  do
15:        Compute  $\mu_{m,c}$  and  $\Sigma_{m,c}$  to parameterize  $\mathcal{N}_{m,c}$ 
16:      end for
17:      Send parameters  $\theta_m^t$  and Gaussians  $\mathcal{N}_{m,c}$  to the server
18:    end for
19:   Server side:
20:     Compute  $\theta^t = \frac{1}{|D^t|} \sum_{m=1}^M |D_m^t| \theta_m^t$ 
21:     for each class  $c \in C^t$  do
22:       Compute  $\tilde{Q}_c = \sum_{m=1}^M \pi_{m,c} \mathcal{N}_{m,c}(\mu_{m,c}, \Sigma_{m,c})$ 
23:     end for
24:     Compute  $\tilde{Q} = \sum_{c=1}^C \omega_c \tilde{Q}_c$ 
25:     Collect dataset  $\hat{D}$  by sampling feature vectors from  $\tilde{Q}$ 
26:     for each rebalancing epoch  $e \in \{1, \dots, E_r\}$  do
27:       Optimize  $W$  using equation 7 (main paper)
28:     end for
29:   end for

```
